Patterning with Magnetic Materials at the Micron Scale

Serge Palacin,[†] Pirmin C. Hidber,[†] Jean-Philippe Bourgoin,[‡] Corinne Miramond,[§] Claude Fermon,[§] and George M. Whitesides*,[†]

Department of Chemistry, Harvard University, 12 Oxford Street, Cambridge, Massachusetts 02138; Service de Chimie Moléculaire, Commissariat à l'Energie Atomique, Centre d'Etudes de Saclay, 91191 Gif sur Yvette Cedex, France; and Service de Physique de l'Etat Condensé, Commissariat à l'Energie Atomique, Centre d'Etudes de Saclay, 91191 Gif sur Yvette Cedex, France

Received December 7, 1995. Revised Manuscript Received April 1, 1996[⊗]

This paper demonstrates the use of microcontact printing (μCP) and capillary filling (CF) to pattern the deposition of iron oxides on a surface with feature sizes of microns. Selective wetting of both self-assembled monolayers (SAMs) of alkanethiolates on gold and alkylsiloxanes on Si/SiO_2 formed by microcontact printing limited the deposition of the iron oxides to the hydrophilic areas on the surfaces; thereby, the chemical functionality of the hydrophilic SAM had only a minor influence on the wetting behavior and the deposition. The iron oxides were deposited either as magnetite particles from colloidal solution, by precipitation of the oxide from previously deposited drops of water containing an iron(III) salt, or by ferrite plating. The size of the metal oxide patterns was limited to the size of the areas that could be patterned using μCP. Capillary filling using a colloidal solution of magnetite could also be used to fabricate continuous, interconnected structures of magnetite. The magnetic properties of the deposited iron oxides were characterized by magnetic force measurement (MFM) and by measurement of the magnetization. The magnetite particles deposited in these experiments showed superparamagnetic behavior; they were too small individually to support a permanent magnetization.

Introduction

This paper describes the use of microcontact printing (μCP)[1−3] and capillary filling (CF)[4] to control and direct the deposition of metal oxides on various substrates at the micron scale. Microcontact printing (μCP)[1−3] is a broadly applicable technique for derivatizing surfaces: patterns having dimensions less than 0.5 μm can be routinely generated on metals such as gold,[1−3] silver,[5,6] or copper[6,7] and on Si/SiO_2[8−10] by forming self-assembled monolayers (SAMs) using an elastomeric stamp inked with a substance that reacts with the surface. In the case of gold surfaces, alkanethiols are used.[1−3] The autophobicity of the resulting SAMs controls the edge resolution of the patterns.[11] Using different ω-terminated thiols, it is possible to define areas having well-controlled properties on the surface and to accomplish, for example, the selective wetting of designed areas of the surface. Aqueous solutions,[12−15] hydrophobic liquids,[16,17] polymers,[18] or soluble biological material[19−22] can thus be patterned onto solid substrates. Selective wetting can also be used to induce the geometrically defined plating of a conductive polymer.[23] Capillary filling (CF)[4] is an alternative technique for patterning, well suited for the formation of continuous, interconnected features. CF uses an elastomeric stamp with a relief structure. When this stamp is placed on a solid support, a network of capillaries is formed at the interface. A drop of a suitable liquid, placed at one end of the stamp, spontaneously fills the open channels by capillary forces; CF allows the formation of well-defined arrays of polymers, hydrogels, liquid crystals, proteins, or inorganic salts.[4]

In the present work, we demonstrate the use of μCP and CF for the patterning of different substrates with

[†] Harvard University.
[‡] Service de Chimie Moléculaire.
[§] Service de Physique de l'Etat Condensé.
* To whom correspondence should be addressed.
[⊗] Abstract published in *Advance ACS Abstracts,* May 1, 1996.

(1) Kumar, A.; Whitesides, G. M. *Appl. Phys. Lett.* **1993**, *63*, 2002.
(2) Kumar, A.; Biebuyck, H. A.; Whitesides, G. M. *Langmuir* **1994**, *10*, 1498.
(3) Wilbur, J. L.; Kumar, A.; Kim, E.; Whitesides, G. M. *Adv. Mater.* **1994**, *6*, 600.
(4) Kim, E.; Xia, Y.; Whitesides, G. M. *Nature* **1995**, *376*, 581.
(5) Xia, Y.; Kim, E.; Whitesides, G. M. *J. Electrochem. Soc.*, in press.
(6) Xia, Y.; Zhao, X.-M.; E., K.; Whitesides, G. M. *Chem. Mater.* in press.
(7) Xia, Y.; E., K.; Mrksich, M.; Whitesides, G. M. *Chem. Mater.* submitted.
(8) Xia, Y.; Mrksich, M.; Kim, E.; Whitesides, G. M. *J. Am. Chem. Soc.* **1995**, *117*, 9576.
(9) Jeon, N. L.; Nuzzo, R. G.; Xia, Y.; Mrksich, M.; Whitesides, G. M. *Langmuir* **1995**, *11*, 3024.
(10) Jeon, N. L.; Clem, P. G.; Nuzzo, R. G.; Payne, D. A. in press.
(11) Biebuyck, H. A.; Whitesides, G. M. *Langmuir* **1994**, *10*, 4581.
(12) Lopez, G. P.; Biebuyck, H. A.; Frisbie, C. D.; Whitesides, G. M. *Science* **1993**, *260*, 647.
(13) Bunker, B. C.; Rieke, P. C.; Tarasevich, B. J.; Campbell, A. A.; Fryxell, G. E.; Graff, G. L.; Song, L.; Liu, J.; Virden, J. W.; McVay, G. L. *Science* **1994**, *264*, 48.
(14) Rieke, P. C.; Tarasevich, B. J.; Wood, L. L.; Engelhard, M. H.; Baer, D. R.; Fryxell, G. E.; John, C. M.; Laken, D. A.; Jaehnig, M. C. *Langmuir* **1994**, *10*, 619.
(15) Abbott, N. L.; Whitesides, G. M. *Langmuir* **1994**, *10*, 1493.
(16) Biebuyck, H. A.; Whitesides, G. M. *Langmuir* **1994**, *10*, 2790.
(17) Gorman, C. B.; Biebuyck, H. A.; Whitesides, G. M. *Chem. Mater.* **1995**, *7*, 252.
(18) Kim, E.; Whitesides, G. M.; Lee, L. K.; Smith, S. P.; Prentiss, M. *Adv. Mater.*, in press.
(19) Stenger, D. A.; Georger, J. H.; Dulcey, C. S.; Hickman, J. J.; Rudolph, A. S.; Nielsen, T. B.; McCort, S. M.; Calvert, J. M. *J. Am. Chem. Soc.* **1992**, *114*, 8435.
(20) DiMilla, P. A.; Folkers, J. P.; Biebuyck, H. A.; Härter, R.; Lopez, G. P.; Whitesides, G. M. *J. Am. Chem. Soc.* **1994**, *116*, 2225.
(21) Singhvi, R.; Kumar, A.; Lopez, G. P.; Stephanopoulos, G. N.; Wang, D. I. C.; Whitesides, G. M.; Ingber, D. E. *Science* **1994**, *264*, 696.
(22) Mrksich, M.; Whitesides, G. M. *Trends Biotechnol.* **1995**, *13*, 228.
(23) Gorman, C. B.; Biebuyck, H. A.; Whitesides, G. M. *Chem. Mater.* **1995**, *7*, 526.

S0897-4756(95)00587-4 CCC: $12.00

metal oxides. Iron oxides were chosen as model compounds. We have used four strategies for the deposition of the iron oxides. First, we used selective wetting for the deposition of magnetite from a colloidal solution on a SAM that had previously been patterned into hydrophobic and hydrophilic areas. Second, we used the same methodology to deposit aqueous drops of an iron(III) salt onto a patterned surface and precipitated the oxide onto the surface from these drops by changing the pH in the droplets. Third, we used CF to build continuous structures of metal oxides. Fourth, we used electroless ferrite plating to build metal oxide structures on a patterned surface.[24−29] In contrast to the other three techniques, ferrite plating, in principle, allows the metal oxide film to be grown progressively to a desired value of thickness. The magnetic properties of the deposited iron oxides were investigated by magnetic force microscopy (MFM) and by the characterization of their magnetic behavior.

Experimental Section

General Techniques. All chemicals were reagent grade and used as received, with the exception of hexadecanethiol, which was distilled before use. Hexadecanethiol (HDT), 2-aminoethanethiol hydrochloride (AET, $HSCH_2CH_2NH_3Cl$), dithiothreitol (DTT, $HSCH_2CH(OH)CH(OH)CH_2SH$), potassium thioacetate (PTA, CH_3COSK), 3-mercaptopropionic acid (MPA, $HSCH_2CH_2COOH$), 2-mercaptoethanesulfonic acid sodium salt (MES, $HSCH_2CH_2SO_3Na$), and octadecyltrichlorosilane (OTS, $C_{18}H_{37}SiCl_3$) were obtained from Aldrich. Gold (99.999%) and titanium (99.99%) were obtained from Materials Research Corp.

Stamps were prepared as described previously[1] from poly(dimethylsiloxane) (PDMS: Sylgard 184, Dow Corning). Silicon substrates were n-type semiconductor grade silicon ⟨100⟩ wafers (2 in. diameter) from Silicon Sense Inc. They were cleaned just before use by dissolving the SiO_2 layer using a 30 s dip in a 5 M HF + 1 M NH_4F aqueous solution, followed by reoxidation of the silicon surface with a 30 min treatment with "piranha solution" (7:3 v/v mixture of concentrated H_2SO_4 and 30% H_2O_2). *CAUTION: Piranha solution reacts violently with many organic materials and should be handled with extreme care.* Glass slides (microslides, VWR Scientific Inc.) were cleaned directly with the piranha solution. The substrates were then thoroughly rinsed with deionized water and dried under nitrogen.

Gold films were formed by e-beam evaporation of ≈2 nm of titanium (adhesion promoter) and ≈20 nm of gold onto a silicon wafer.

Synthesis of the Colloidal Suspensions of Magnetite. The stabilization of particles of metal or metal oxides,[30,31] including magnetically active particles (either hematite, Fe_2O_3, or magnetite, Fe_3O_4) can be successfully achieved in aqueous solutions[32−34] or in a polymer.[35−38] The procedure we followed generated surfactant-free colloidal suspensions in water of both positively and negatively charged particles stabilized by repulsive double-layer interactions. The colloidal suspensions of magnetite were prepared as described before.[32] Typically, a mixture of 40 mL of 1 M $FeCl_3$ and 10 mL of 2 M $FeCl_2$ in 2 M HCl was poured into a well-stirred ammonia solution (500 mL of 0.7 M NH_4OH). The black precipitate, which formed instantaneously, was separated by centrifugation. For the preparation of a stable suspension of anionic particles, the precipitate was stirred for 30 min with a concentrated solution (1 M) of tetramethylammonium hydroxide using aspirator vacuum to remove excess ammonia. After centrifugation, the final black solid was suspended in the minimum amount (15−20 mL) of pure water. This suspension (which we will call **Mag**$^-$ in the following text) was stable for several weeks, although shaking was necessary to resuspend settled particles. For the preparation of a stable suspension of cationic particles, the black precipitate was washed for 15 min with 3 M $HClO_4$, separated by centrifugation, and then resuspended in the minimum amount of pure water. This suspension (which we will call **Mag**$^+$) could be stored only for a few days because the iron oxide slowly dissolved in the acidic medium. Examination of the particles of **Mag**$^+$ and **Mag**$^-$ by TEM indicated they were similar in size and composition. The relative average surface charge of **Mag**$^+$ and **Mag**$^-$ was reported between 0.02 and 0.03 electron/iron.[32] The size of the particles was between 5 and 12 nm; electron diffraction proved that the particles were magnetite (Fe_3O_4, JCPDC File No. 19-629) in both cases. Both suspensions behaved as ferrofluids in the presence of a magnetic field. No difference was observed between the behavior of these suspensions and a commercial ferrofluid (EMG 705, Ferrofluidics, Nashua, NH) in a magnetic field.

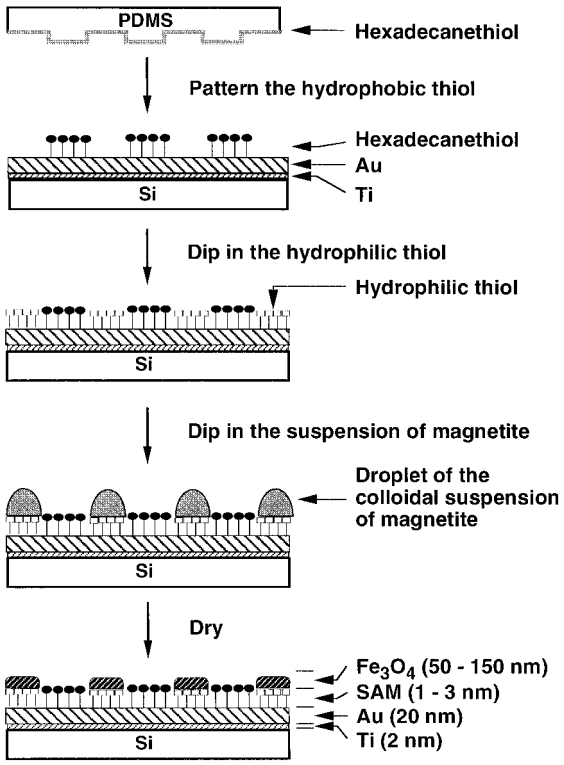

Figure 1. General procedure for using μCP to pattern gold films with colloidal magnetite (Fe_3O_4). The gold sample was first patterned with hexadecanethiol by μCP and then dipped into a solution of a hydrophilic thiol (e.g., 2-aminoethanethiol hydrochloride, dithiothreitol, potassium thioacetate, mercaptopropionic acid, or 2-mercaptoethanesulfonic acid sodium salt) to derivatize the remaining areas of bare gold. The sample was then immersed in the colloidal suspension of magnetite for 15 s, before drying either in air or at 60 °C for 12 h or in vacuum at 200 °C for 2 h.

Patterning with Magnetic Materials via Selective Wetting. Figure 1 outlines the general procedure we used for patterning with magnetic materials based on selective

(24) Abe, M.; Tamaura, Y., *J. Appl. Phys.*, **1984**, *55*, 2614.
(25) Abe, M.; Tanno, Y.; Tamaura, Y. *J. Appl. Phys.* **1985**, *57*, 3795.
(26) Tamaura, Y.; Tanno, Y.; Abe, M. *Bull. Chem. Soc. Jpn.* **1985**, *58*, 1500.
(27) Abe, M.; Tamaura, Y.; Goto, Y.; Kitamura, N.; Gomi, M. *J. Appl. Phys.* **1987**, *61*, 3211.
(28) Itoh, T.; Hori, S.; Abe, M. *J. Appl. Phys.* **1991**, *69*, 5911.
(29) Abe, M.; Itoh, T.; Tamaura, Y. *Thin Solid Films* **1992**, *216*, 155.
(30) Matijevic, E. *Langmuir* **1986**, *2*, 12.
(31) Ocana, M.; Rodriguez-Clemente, R.; Serna, C. J. *Adv. Mater.* **1995**, *7*, 212.
(32) Jolivet, J. P.; Massart, R.; Fruchart, J. M. *Nouv. J. Chim.* **1983**, *7*, 325.
(33) Zhao, X. K.; Herve, P. J.; J. H. F. *J. Phys. Chem.* **1989**, *93*, 908.
(34) Sugimoto, T.; Matijevic, E. *J. Colloid Interface Sci.* **1980**, *74*, 227.
(35) Wooding, A.; Kilner, M.; Lambrick, D. B. *IEEE Trans. Magn.* **1988**, *24*, 1650.
(36) Yokoi, H.; Yagishita, K.; Nakanishi, Y. *Bull. Chem. Soc. Jpn.* **1990**, *63*, 746.

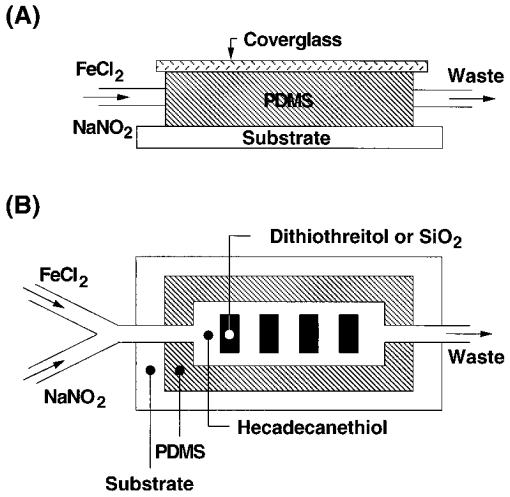

Figure 2. Experimental setup for the deposition of magnetite from solution. The patterned substrate was mounted in a flow-through cell; the cell is shown in side view (A), and in top view (without coverglass) (B). The aqueous solution of $FeCl_2$ and $NaNO_2$ (kept at 70 °C and under nitrogen) were supplied using two peristaltic pumps; they were mixed just before they reached the substrate. The whole cell was immersed in a water bath to keep the temperature at 70 °C.

wetting of the substrate surface. The surface of the substrates were derivatized using μCP.

Patterning Magnetite by Ferrite Plating in Aqueous Solution. The deposition of magnetite on patterned substrates from aqueous solution has been performed according to the procedure of Abe et al.[27] The substrate was mounted in a flow-through cell (Figure 2). Typically, a 10 mM solution of $FeCl_2$ (degassed under vacuum, buffered at pH 7 with 65 mM NH_4OAc, 70 °C, under N_2) and a 30 mM solution of sodium nitrite (degassed under vacuum, 70 °C, under N_2) were allowed to flow over the surface of the substrate. The two solutions were supplied in a ratio of $FeCl_2$ to $NaNO_2$ of 10:1 (v/v). The substrates were either gold films patterned with a hydrophobic and a hydrophilic thiol or gold films selectively etched to give access to the supporting silicon wafer. The continuous flow of reactants was maintained for 10−30 min, and the samples were then thoroughly rinsed with water and dried under a flow of nitrogen.

Instrumentation. Scanning electron microscopy (SEM) was carried out using a JEOL JSM-6400 instrument. Atomic force microscopy (AFM) used a Topometrix TMX 2010 scanning probe microscope. The images were obtained using a cantilever made from silicon nitride in constant contact with the surface. Data were collected in the forward part of the scan. Transmission electron microscopy (TEM) of the colloidal suspensions of magnetite were obtained on a Phillips EM 420 microscope.

Magnetic force microscopy (MFM) images were obtained on a Nanoscope III (Digital Instruments, Santa Barbara, CA) scanning probe system with a Multimode TM system microscope. The probes were single-crystal silicon cantilevers (225 μm) with pyramidal tips coated with a Co−Cr alloy (MESP tips available from DI). Magnetization curves were measured using a superconducting quantum interference device magnetometer (SQUID) from Cryogenic Ltd.

Results and Discussion

Micron-Scale Patterned Magnetic Thin Films Can Be Obtained from Colloidal Suspensions of Magnetite by Selective Wetting. The deposition of the magnetite particles on the substrate was accomplished according to the procedure outlined in Figure 1. The substrate was a thin film of gold supported on a titanium-primed silicon wafer. The pattern was transferred from the elastomeric stamp (PDMS) onto the gold surface via selective deposition of hexadecanethiol (HDT). The stamp was inked with a 10^{-3} M solution of HDT in ethanol and then left in contact with the gold surface for 15 s. The stamp was removed and the sample was dipped for 30 s into an ethanolic solution of the hydrophilic thiol in order to create the hydrophilic areas that could be wetted by the aqueous colloidal suspension of magnetite. After rinsing with ethanol and drying under a flow of nitrogen, the sample was dipped into a suspension of either positively (**Mag**$^+$) or negatively (**Mag**$^-$) charged colloidal magnetite particles for 15 s and then pulled from the suspension. The water was allowed to evaporate from the patterned surface by drying in open air, in an oven at 60 °C overnight, or at 200 °C in vacuum for 2 h.

Figure 3A,B shows the results obtained after dipping a gold substrate patterned with hexadecanethiol (HDT) and 2-mercaptoethanesulfonic acid sodium salt (MES) into the two types of magnetic suspensions. These colloidal suspensions generated almost flat regions of magnetite; the films filled the hydrophilic areas almost completely. Some shrinkage (≈30% in area with respect to the area covered by the colloidal solution after the dewetting) occurred upon drying at 200 °C for 2 h, and the square shape was sometimes lost. The average area of the dried magnetite films was ≈60% of the area of the original hydrophilic area;[39] their thickness was between 50 and 100 nm (Figure 3D). Micron-scale dots could easily be achieved using the cationic colloidal suspension **Mag**$^+$. In contrast, the suspension **Mag**$^-$ did not always wet the hydrophilic areas when they were smaller than ≈4 μm^2. We hypothesize that this discrepancy between the two colloidal suspensions resulted from the higher viscosity of our anionic suspension, which prevented clean, selective dewetting of the hydrophilic areas when the gold film supporting the patterned SAM was pulled from the suspension.

Composition of the Hydrophilic SAM Influences but Does Not Govern the Wetting of the Monolayer with the Magnetic Precursor. Five different hydrophilic thiols were tested as substrates to promote the wetting of the monolayer with the precursor of the magnetic solid. All were short-chain thiols, in order to avoid any replacement of the hexadecanethiol during the formation of the hydrophilic areas.[40] Our set of hydrophilic thiols was selected in order to assess the role of ionic, protic and polar interactions. We used a cationic thiol (2-aminoethanethiol hydrochloride, AET), an anionic thiol (2-mercaptoethanesulfonic acid sodium salt, MES), an ionizable thiol (3-mercaptopropionic acid, MPA), a neutral protic thiol (dithiothreitol, DTT), and a neutral polar thiol (potassium thioacetate, PTA). Figure 4 shows that suspensions of both **Mag**$^+$ and

(37) Elkafrawy, S.; Hoon, S. R.; Lambrick, D. B.; Bissell, P. R.; Price, C. *IEEE Trans. Magn.* **1990**, *26*, 1846.
(38) Nguyen, M. T.; Diaz, A. F. *Adv. Mater.* **1994**, *6*, 858.

(39) The 30% were counted with respect to the original covered area. It is the decrease in size of each dot, whatever area of the hydrophilic region. The 60% were determined with respect to the area of the hydrophilic SAM; this means that the colloidal suspensions did not cover the entire hydrophilic area after dewetting.
(40) Short-chain thiols do not replace long-chain thiolates in SAMs on gold. Bain, C. D.; Biebuyck, H. A.; Whitesides, G. M. *Langmuir* **1989**, *5*, 723. Chidsey, C. E. D.; Bertozzi, C. R.; Putvinski, T. M.; Mujsce, A. M. *J. Am. Chem. Soc.* **1990**, *112*, 4301. Collard, D. M.; Fox, M. A. *Langmuir* **1991**, *7*, 1192. Folkers, J. P.; Laibinis, P. E.; Whitesides, G. M. *Langmuir* **1992**, *8*, 1330. Folkers, J. P.; Laibinis, P. E.; Whitesides, G. M.; Deutch, J. *J. Phys. Chem.* **1994**, *98*, 563. Rowe, G. K.; Creager, S. E. *Langmuir* **1994**, *10*, 1186.

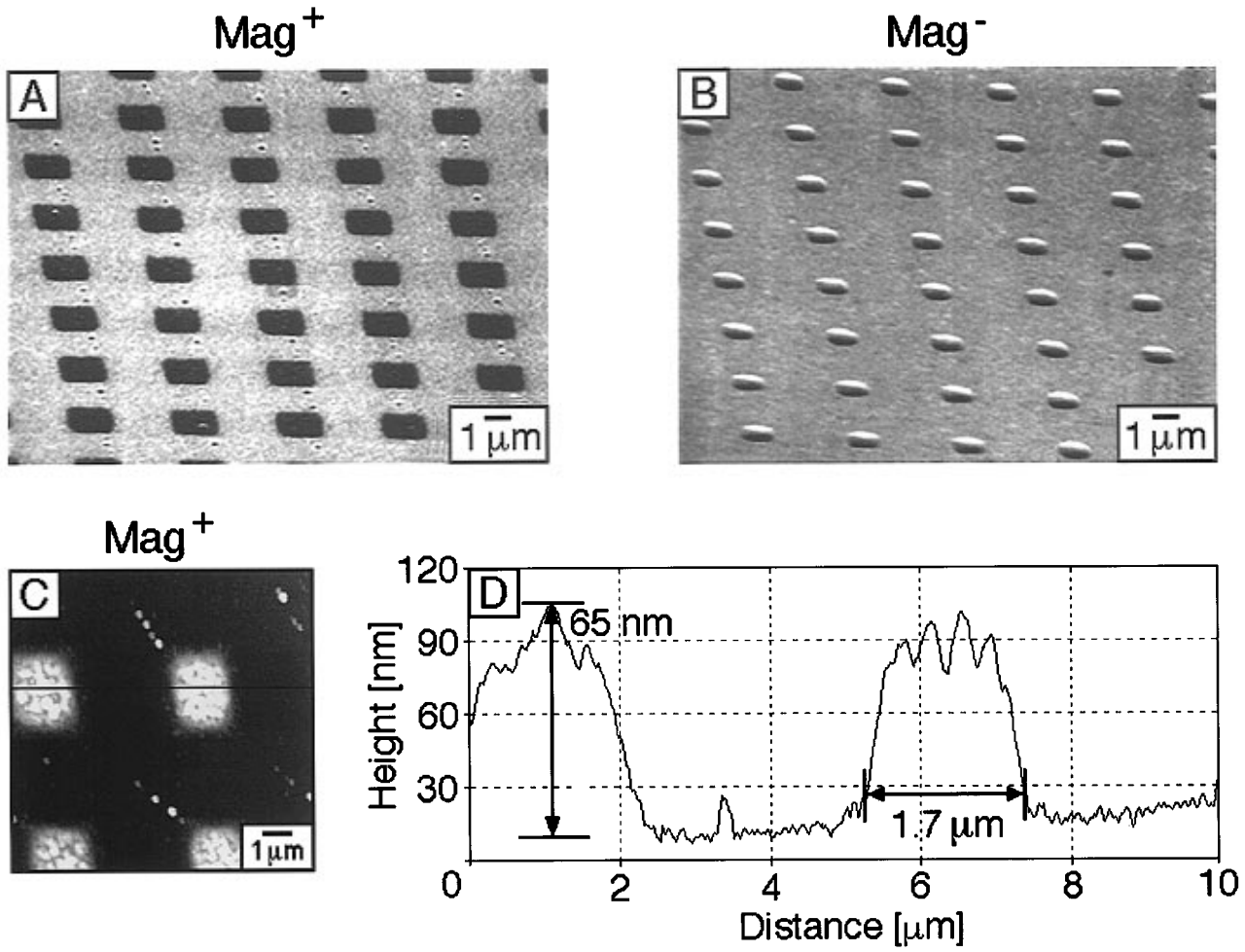

Figure 3. SEM pictures of magnetite dots on a sample patterned with hexadecanethiol and 2-mercaptoethanesulfonic acid sodium salt. The magnetite dots were obtained by selective wetting of the hydrophilic areas of the sample (A) with a suspension of **Mag**$^+$ and (B) with a suspension of **Mag**$^-$. (C) AFM topography image recorded on a sample patterned with hexadecanethiol and 2-mercaptoethanesulfonic acid sodium salt with **Mag**$^+$; (D) height profile of the sample shown in (C).

Mag$^-$ deposited successfully on each of these hydrophilic thiols except on MPA (not shown), which gave only partially, poorly defined depositions on the hydrophilic areas. Although the deposition was more efficient on the charged thiols than on the neutral ones, even DTT gave significant deposition. These results suggest that the deposition was mainly governed by the selective wetting of the hydrophilic areas; long-range double-layer electrostatic interactions between particles and surface groups of the monolayer had only a limited influence. The primary interaction that occurred during the deposition was probably between the hydrophilic heads of the short-chain thiols and water rather than directly between the charged magnetite particles and the polar head groups of the hydrophilic thiolates. Direct interactions may have occurred later, during drying or heating. This inference is strengthened by the apparent absence of specific electrostatic interactions between the colloidal particles and the thiols. **Mag**$^-$ and **Mag**$^+$ behaved in almost the same way regardless of the structure of the hydrophilic monolayer: **Mag**$^+$ always filled the entire hydrophilic area and gave a very low shrinkage upon drying; **Mag**$^-$ exhibited large shrinkage upon drying and gave rise to round shapes or square shapes with round corners. The loss in shape of the deposited areas also demonstrates the weakness of the particle/surface interactions: the particles were confined within the aqueous droplets, followed their symmetrical shrinkage upon drying until the concentration of the suspension was high enough for their precipitation and settlement, regardless of the nature of the hydrophilic SAM. The shape thus results from the behavior of the entire deposited droplet on the corresponding SAM, rather than from direct electrostatic interactions between the SAM and the particles.

Micron-Scale Magnetic Areas Can Be Obtained via Precipitation of Iron Salts. Aqueous solutions of iron(III) salts have already been used to generate magnetic materials regions on a substrate, although on fairly large dimensions (10−50 μm).[14] We have successfully applied a similar procedure to produce patterned areas as small as 0.5 μm in width. A gold film, patterned with hydrophobic and hydrophilic areas using μCP was immersed in a solution containing the iron salt and then slowly pulled out of it. To get a precipitation of the iron salt, we placed the selectively wetted sample for 15 min in an ammonia atmosphere. Water was removed by slow drying in the open air, by rapid drying in vacuum at 200 °C for 2 h, or by heating the sample at 60 °C overnight. The deposited material prepared in this way is likely to be iron hydroxide ($Fe(OH)_3$), iron oxyhydroxide (α-FeOOH) or, when heated to higher temperatures, paramagnetic hematite α-Fe_2O_3.[41] The exact mineral formed is sensitive to solution conditions.

(41) Bailar, J. C., Emeleus, H. J., Nyholm, R., Trotman-Dickenson, A. F., Eds. *Comprehensive Inorganic Chemistry*; Pergamnon Press: New York, 1975; pp 1040−1041.

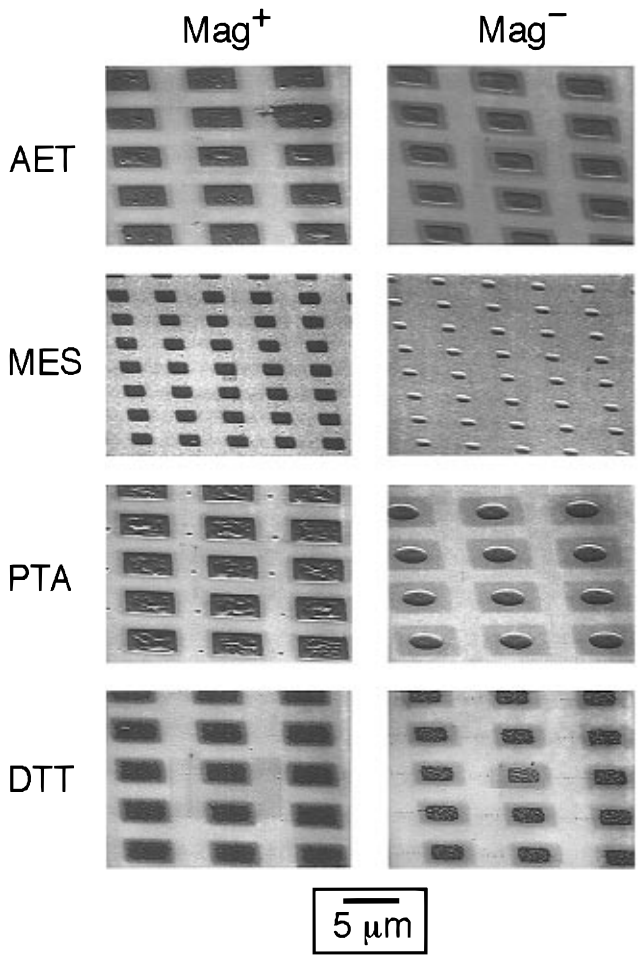

Figure 4. SEM pictures of the magnetite dots deposited from **Mag**$^+$ and **Mag**$^-$ on four different hydrophilic SAMs. The type of magnetic suspension (**Mag**$^+$ or **Mag**$^-$) is given in the top row. The name of the hydrophilic thiol is given in the left column (AET, 2-aminoethanethiol hydrochloride; MES, 2-mercaptoethanesulfonic acid sodium salt; PTA, potassium thioacetate; DTT, dithiothreitol).

Since we have not determined the exact phase composition of the precipitates, we will refer to them simply as "iron oxyhydroxides" in the following text.

Figure 5 shows examples of the patterned areas generated by this technique. Upon heating, some shrinkage of the initially deposited material occurred, consistent with the evaporation of excess water from the rapidly precipitated iron hydroxide. We used saturated aqueous solutions of $Fe(NO_3)_3$ as the fluid phase. Figure 5A,B shows that an homogeneous, lenslike depositions was obtained with an almost perfect selectivity for the hydrophilic regions of the substrate. Figure 5D gives the height profile measured by AFM on the dots prepared from $Fe(NO_3)_3$. The average thickness of these dots was about three times higher than that observed with **Mag**$^+$ or **Mag**$^-$. The SEM and AFM pictures confirm that the deposition of each rounded dot filled about one-fourth of the entire hydrophilic area defined by the patterning. Upon drying, the iron oxyhydroxides dots derived from $Fe(NO_3)_3$ kept their shape by decreasing the area of contact with the hydrophilic SAM.

Direct Deposition on Silicon Dioxide Is Possible but Is Less Effective Than on Gold. To study the high-temperature behavior of the patterned oxides, it was necessary to pattern surfaces other than gold (for example the silicon dioxide layer on silicon). We have used μCP to generate isolated areas of silicon dioxide in a gold substrate by using hydrophobic, patterned SAMs as a resist for etching the gold. This procedure has been described previously and can lead to either flat or hollow regions of silicon dioxide, separated from each other by areas of gold covered by a hydrophobic thiol.[2,3,42]

Figure 6A shows the iron oxyhydroxides deposited on squares of silicon dioxide by treatment of an aqueous solution of $Fe(NO_3)_3$ with ammonia. Each area of silicon dioxide (in black on the picture) bears one piece of iron oxyhydroxides, which exhibits no specific shape or position within the boundaries of the hydrophilic region of SiO_2. On the same substrate, the colloidal suspensions of magnetite **Mag**$^+$ and **Mag**$^-$ gave rise to very poorly defined depositions in the regions of silicon dioxide. Using the same method, we could also achieve selective deposition of iron oxyhydroxides on silicon dioxide surfaces without any previous coverage with gold. A silicon dioxide surface was patterned by μCP with octadecyltrichlorosilane.[8,9] The unstamped, hydrophilic regions of the silicon dioxide were selectively wetted with a $Fe(NO_3)_3$ solution. We applied the same technique to direct the deposition of the iron oxyhydroxides into the holes of patterned silicon surface (Figure 6B). After etching an array of holes with the shape of an inverted pyramid into the Si/SiO_2 surface,[2,3,42] we covered the flat upper parts of the sample with an octadecylsilane monolayer[8,9] by μCP with a flat PDMS stamp. The iron oxyhydroxides particles were precipitated by the treatment with ammonia of the droplets of aqueous solutions of $Fe(NO_3)_3$ that had been deposited into the holes by selective wetting. The sample was dried at 200 °C for 2 h. Figure 6B shows that each pyramidal hole contains its own irregular patch (or patches) of iron oxyhydroxides.

Continuous, Interconnected Features of Magnetic Materials Can Be Fabricated by Capillary Filling. Although selective wetting could easily be applied to the formation of continuous features (Figure 7), the results (at least for patterns with small widths) were not as good as for closed domains. The main reason for that difference was clearly the shrinkage that occurred on drying of the wet pattern derived from the selective wetting. When the hydrophilic area was small enough, the shrinkage broke the continuity of the iron oxide pattern.

Capillary filling (CF) is an alternative technique that often works well in the formation of continuous features. Figure 8 shows a continuous star pattern built with **Mag**$^-$ on a glass substrate. The elastomeric stamp with the star pattern was placed on the substrate. Immediately after a drop of **Mag**$^-$ was placed at one end of the stamp, the open channels filled spontaneously by capillary action; approximately 15 min was required to fill capillaries 1 cm long. The picture shows only a small, selected area of the substrate. The uniformity of the results was poor. Even with larger patterns (50 μm wide lines, for example), not all channels were entirely filled by the suspension. Often, the colloidal suspension reached the end of the channels by traveling along the edges of the polymeric channels; this pattern of filling left the bulk of the channels empty. This effect, in principle, would allow us to fabricate small "wires"

(42) Kim, E.; Kumar, A.; Whitesides, G. M. *J. Electrochem. Soc.* **1995**, *142*, 628.

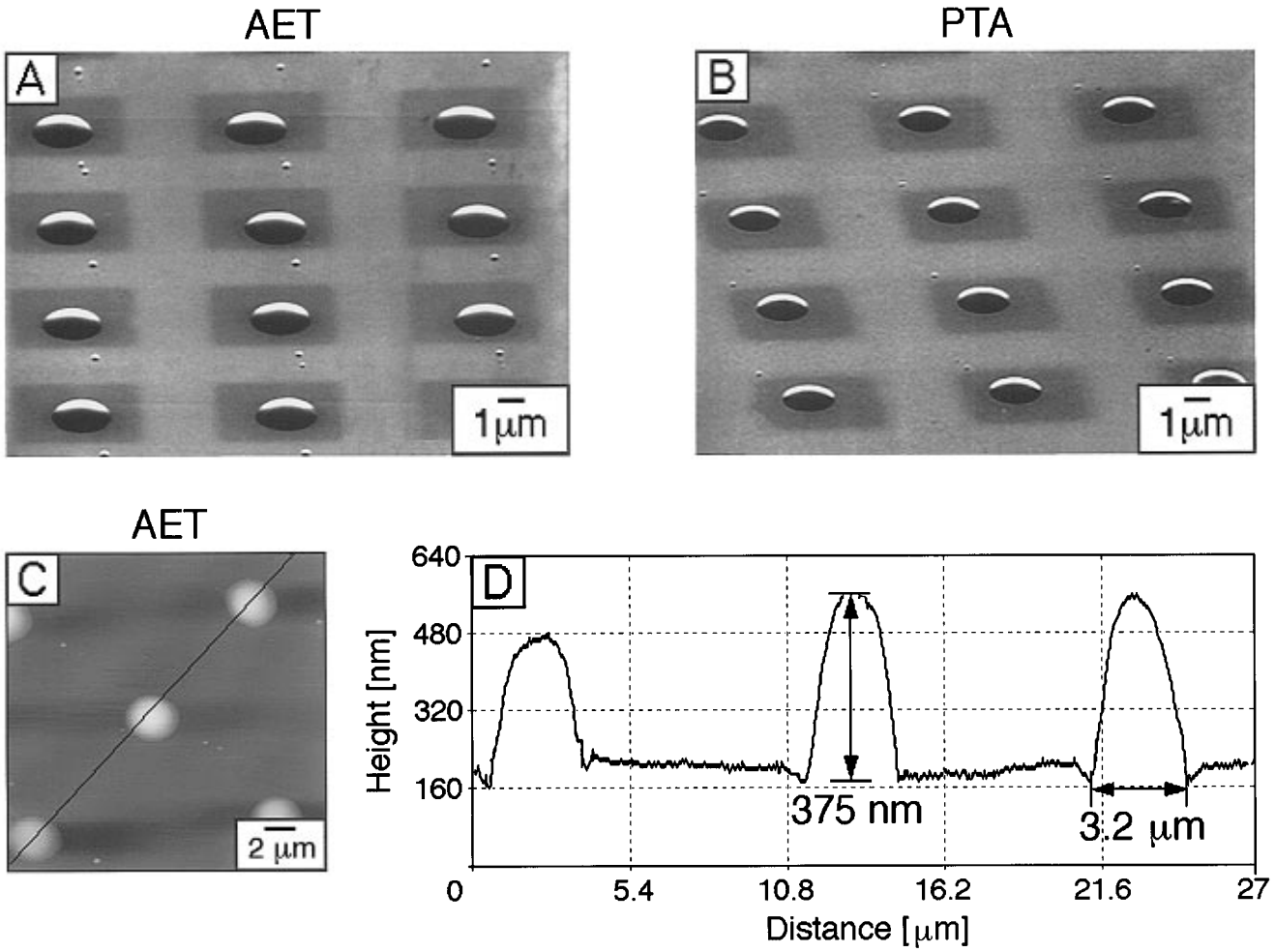

Figure 5. SEM pictures of iron oxyhydroxides dots obtained on a patterned sample by selective wetting of the hydrophilic areas with $Fe(NO_3)_3$ and precipitating the iron oxyhydroxides with ammonia vapor. The substrates were patterned (A) with hexadecanethiol and 1-aminoethanethiol hydrochloride (AET), and (B) with hexadecanethiol and potassium thioacetate (PTA). (C) AFM topography image recorded on a sample patterned with $Fe(NO_3)_3$ on AET; (D) height profile of the sample shown in (C).

of magnetite but was not developed here for that purpose. Although these results do not represent a technique that can be used reproducibly, they do provide evidence that this technique can work, if it is correctly applied.

Continuous Micron-Scale Magnetic Areas Can Be Obtained by Selective Deposition of Magnetite from Aqueous Solution. Magnetite and ferrites can be successfully deposited from solutions of iron(II) salts at low temperatures (<90 °C) by electroless or chemical ferrite plating.[24−29] In contrast to the electro ferrite-plating, the chemical ferrite plating uses oxidizing reagents rather than an anodic current and can be applied to deposit spinel films of various compositions on conducting and nonconducting substrates.[25] Good adhesion of the deposited ferrite film is achieved on hydroxylated surfaces such as glass, metal oxides, or plasma-treated polymers but not on hydrophobic surfaces.[25] We have applied this process to the selective deposition of magnetite on substrates that had been previously patterned by μCP.

Gold films were derivatized by stamping with hexadecanethiol (HDT) and then filling the remaining bare gold areas with dithiothreitol (DTT). We chose DTT because it offers to the plating solution a hydroxyl-terminated surface similar to that of silicon dioxide. An aqueous solution of $FeCl_2$ was continuously pumped over the patterned substrate surface (Figure 2). The oxidizing reagent, an aqueous solution of sodium nitrite, was added to the $FeCl_2$ solution just before it reached the substrate. A continuous flow of the two reactants was maintained for 10−30 min. The sample was then thoroughly rinsed with water and dried under a flow of nitrogen. Figure 9A shows the result of the selective deposition of magnetite on patterned surfaces. The adhesion of the ferrite film was high on the areas derivatized with DTT, we presume because covalent bonds formed between the oxygen atoms of the DTT molecules and the iron atoms coming from the solution.[25] By contrast, the HDT derivatized areas were resistant to deposition. Micron-scale deposition (e.g., 1-μm^2 squares or 1.5-μm-wide lines) could easily be produced. This technique is particularly efficient for preparing continuous features (which are difficult to build using the wetting technique described in the previous paragraph) because no dewetting of the hydrophilic areas is necessary: the magnetite thin film is grown progressively from the solution upon partial oxidation of the iron(II) salt.

The electroless plating of ferrite is also efficient on silicon dioxide regions made by selective etching of a gold film deposited on silicon.[2,3,42] Figure 9B,C shows SEM pictures of magnetite deposited on a pattern of silicon dioxide surrounded by a gold film covered by an hydrophobic SAM. The deposition of the magnetite showed a high selectivity for the hydrophilic silicon

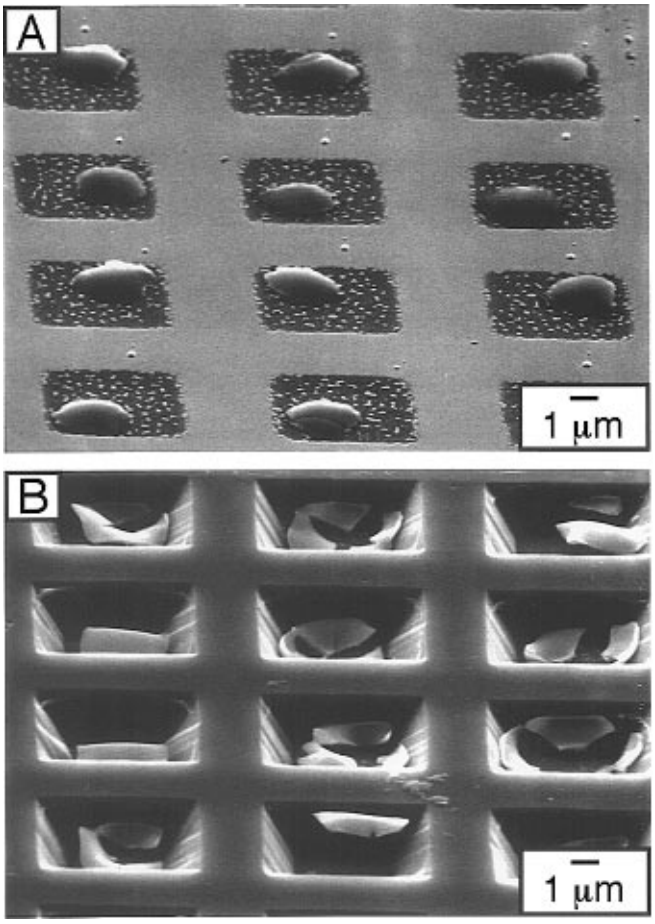

Figure 6. (A) SEM picture of the iron oxyhydroxides deposited on silicon dioxide after selective etching of gold on a patterned gold film and selective wetting of the silicon dioxide areas with $Fe(NO_3)_3$. (B) SEM picture of the iron oxyhydroxides deposited in pits of silicon dioxide etched in Si; the $Fe(NO_3)_3$ solution selectively wetted the SiO_2 surface of these pits. The top, flat regions had been protected and rendered hydrophobic by a monolayer of octadecylsiloxane.

dioxide. The thickness of the ferrite film, evaluated from the SEM pictures, was ≈400 nm.

A Magnetic Field Applied during the Drying Step Had No Effect on the Shape of the Deposited Dots. Since the colloidal suspensions **Mag**$^+$ and **Mag**$^-$ behaved as ferrofluids, we attempted to modify the shapes of the deposited magnetite dots by applying a constant magnetic field of 0.2 T, perpendicular to the substrate, during the deposition process. The sample (only **Mag**$^-$ on AET was tested) was placed under the magnetic field just after deposition and left to dry in air. No significant effect of the magnetic field was observed.

The Micron-Scale Magnetite Dots Can Be Read by Magnetic Force Microscopy (MFM). To assess the magnetic patterning of the surface, the samples have been studied by MFM.[43,44] Imaging was done in two passes across each raster scan line. On the first pass, the topography was recorded using the "tapping mode".[45] On the second pass, the tip was raised to a selected height (typically 20−25 nm) above the surface

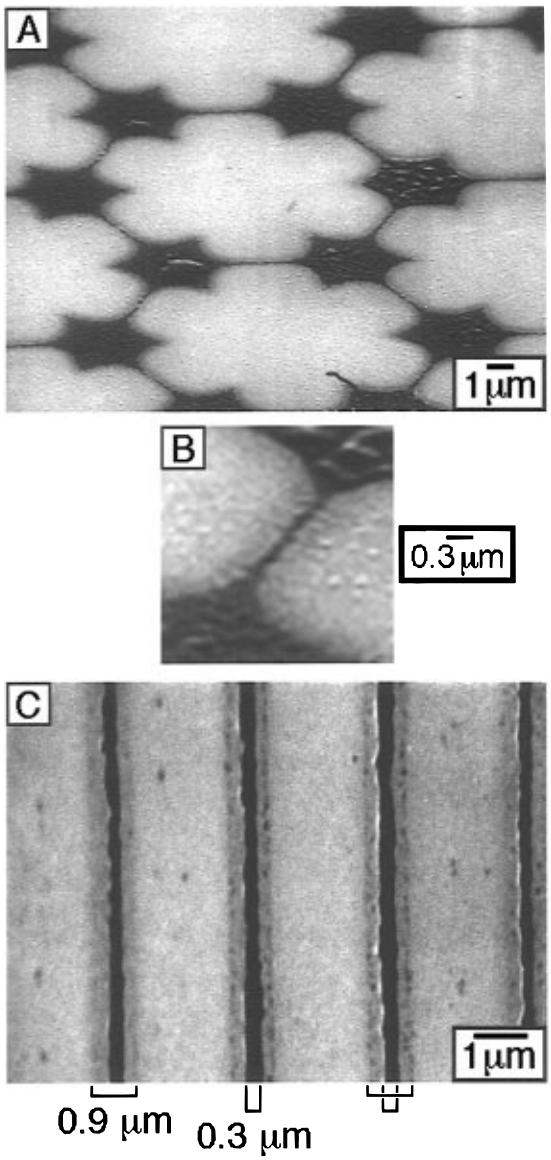

Figure 7. SEM pictures of continuous features of magnetite made by the selective deposition of **Mag**$^+$ on AET areas. The hydrophobic/hydrophilic pattern of HDT and AET on gold was made by μCP. (A) "Star" pattern; the lines between the stars are continuous, as shown in the blowup (B). (C) Lines of magnetite (0.3 μm wide) obtained after drying. The width of the hydrophilic area of AET that was originally wetted by **Mag**$^+$ was about 0.9 μm; the evaporation of water during the drying process resulted in a shrinkage of the line width to about 0.3 μm.

and followed the topography previously recorded on the sample; resonance shifts of the cantilever oscillations (caused by the gradient in the magnetic force on the tip) were then recorded.[46] This procedure made it possible to obtain purely magnetic information on the second pass. Figure 10 shows representative images of the

(43) Babcock, K.; Dugas, M.; Manalis, S.; Elings, V. *Magnetic Force Microscopy: Recent Advances and Applications*; in Demczyk, B. G., Garfunkel, E., Clemens, B. M., Williams, E. D., Cuomo, J. J., Eds.; Materials Research Society: Pittsburgh, PA; pp 311−322.

(44) Gruetter, P. *Applications of Magnetic Force Microscopy*; in Guentherodt, H. J., Anselmetti, D., Meyer, E., Eds.; Kluwer Academic Publisher: Dordrecht; pp 447−470.

(45) In the "tapping mode", the cantilever is oscillated with a high amplitude (≈20 nm) near its resonance frequency and moved toward the surface of the sample until it begins to tap the surface; the topography is obtained directly by measuring the voltage required at the Z piezo to keep the amplitude of the oscillation of the cantilever constant.

(46) The Nanoscope III uses an ac method for magnetic force detection which tracks shifts in the resonance properties (amplitude and phase) of an oscillating cantilever. The resonance frequency is decreased when the magnetic interaction is attractive and increased when it is repulsive. We used the phase detection mode at a constant driving frequency. Resonance shifts give rise to phase shifts which give an image of the magnetic force gradients.

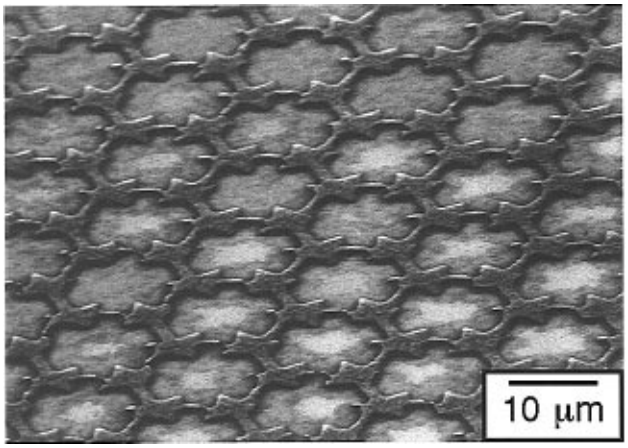

Figure 8. SEM picture of a "star" pattern of magnetite on silicon dioxide fabricated by capillary filling with **Mag**$^-$. The background surface appears partially covered. Almost all the fine lines between the stars are continuous.

topography (A) and the phase shift (B) of a sample patterned with **Mag**$^-$ on AET, recorded with the same magnetic tip. The comparison of the two pictures shows that the pattern imaged in the "topography" mode coincides well with the one imaged in the "phase shift" mode. Regions with deposited **Mag**$^-$ show a smaller phase than the uncovered areas; this observation indicates that the deposited material is magnetically active and interacts attractively with the magnetized tip. The size of the pattern covered with **Mag**$^-$ appeared to be slightly larger (less than 100 nm in each dimension) in the "phase shift" image than the size detected in the "topography" mode. There are two possible reasons for this discrepancy: First, magnetic forces can be detected over a slightly wider range (in distance) than the van der Waals forces responsible for the topographic image, and second, there might be a small drift of the image between the two passes. Images obtained after magnetization of the sample with a magnetic field (15kG) perpendicular to the surface looked comparable to those obtained before the magnetization, except for an increase in the phase shift. No magnetic domains have been seen so far.

We also used the sample shown in Figure 10 (**Mag**$^-$ on AET) to record magnetization curves and to measure the variation of the magnetization with temperature. Figure 11 shows the magnetization curve obtained at 300 K when the magnetic field was cycled between −2 and 2 T. The magnetic field was oriented in the plane of the sample. The magnetization was reversible with a small hysteresis of about 100 G at low field that probably arose from the biggest particles of magnetite. The presence of a small hysteresis shows that the deposited material can not be paramagnetic and confirms the result from the MFM measurements that there are no large magnetic domains.

Figure 12 presents the variation of the magnetization of the sample with temperature in a permanent magnetic field (150 G, with the field axis oriented in the plane of the sample). In the zero field cooling experiment (ZFC), the sample was initially cooled from 300 to 5 K without any applied magnetic field. It was then warmed while applying a 150-G magnetic field, and its magnetization was recorded. In the field cooling experiment (FC), the sample was both cooled and warmed while applying the 150-G magnetic field. The magnetite dots are made of small ferromagnetic particles, which

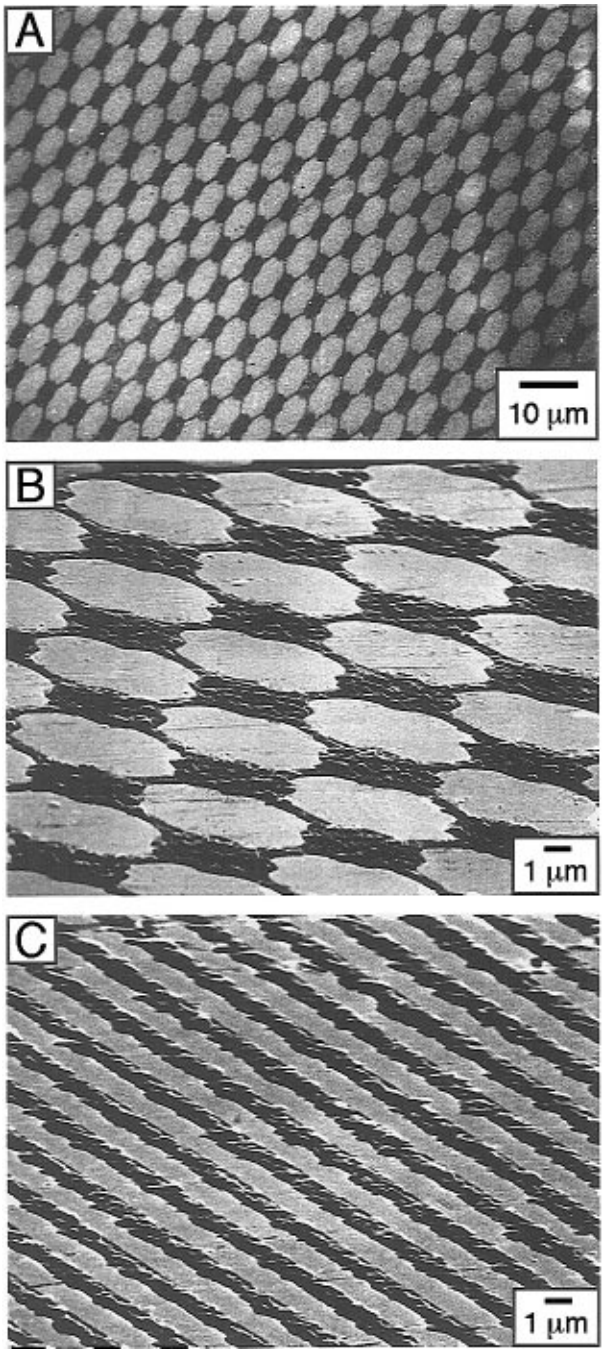

Figure 9. SEM pictures of magnetite patterns obtained by selective electroless deposition of magnetite (A) on the hydrophilic areas of a patterned SAM fabricated using hexadecanethiol and dithiothreitol, and (B, C) on areas of silicon dioxide prepared by selective etching of a patterned gold film.

have a single-domain structure. When one of these particles is magnetized along an easy direction, it remains that way because of the energy of anisotropy. This energy is proportional to the volume of the particle. If this volume is small, thermal fluctuations can be strong enough to flip the direction of magnetization. This is a superparamagnetic behavior. For a given field, the difference between the FC and the ZFC curves gives for each temperature the amount of particles whose energy of anisotropy is higher than the thermal energy. From these curves, we estimate a minimum particle size of 2.5 nm in diameter.[47,48] This figure is compatible

(47) Neel, L. *Ann. Geophys.* **1949**, *5*, 99.
(48) Neel, L. *Philos. Mag. Suppl.* **1955**, *4*, 191.

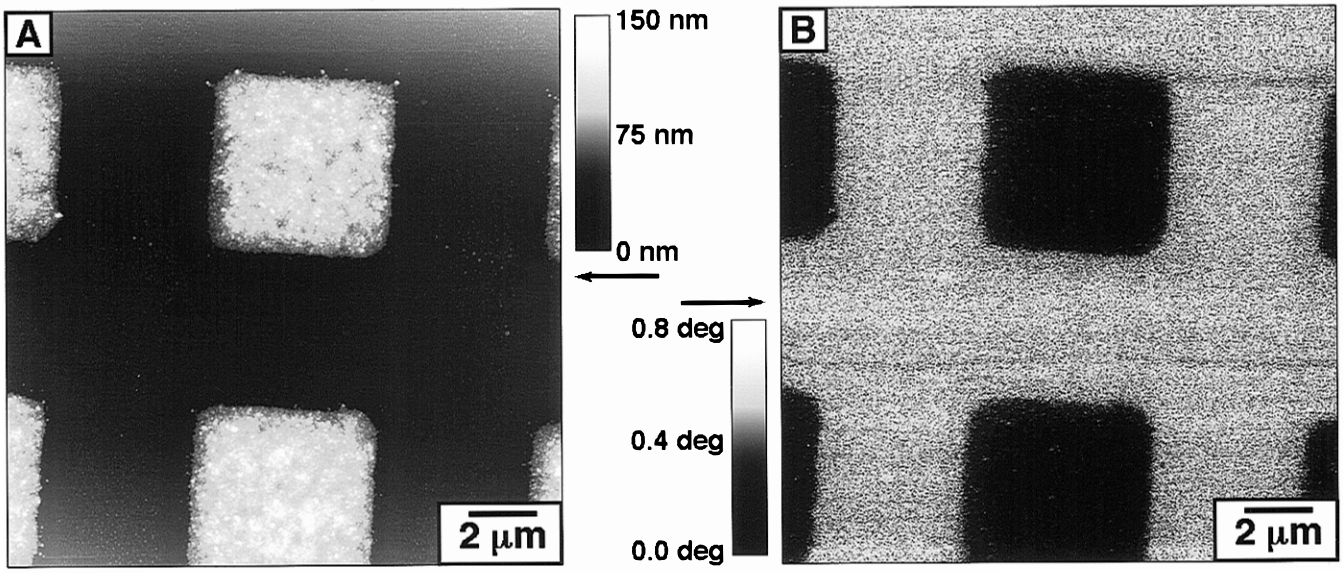

Figure 10. Magnetic force microscopy images of a sample patterned with **Mag**$^-$ on AET. (A) Topography of the sample recorded with a magnetized tip. (B) Phase shifts of the cantilever oscillation recorded by following the previously recorded topography with the magnetic tip.

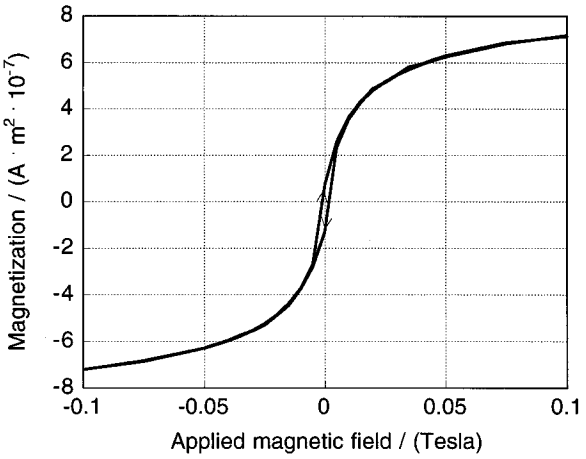

Figure 11. Magnetization curves recorded at room temperature on a sample patterned with **Mag**$^-$ on AET, measured parallel to the film plane. The field was first decreased and then increased. The magnetization has not been normalized to the exact amount of magnetic material in the sample.

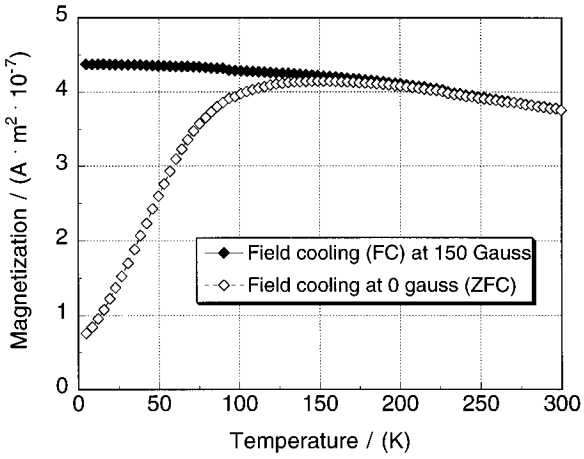

Figure 12. Dependence of the magnetization of a sample patterned with **Mag**$^-$ on AET on temperature. (Field cooling, FC: A magnetic field of 150 G was applied during the cooling and warming of the sample. (Zero field cooling, ZFC: The sample was cooled in the absence of a magnetic field and then warmed with an applied magnetic field of 150 G. The rate of cooling and warming was ca. 25 K/h. Each curve describes only the magnetization recorded when warming the sample.

with our TEM observations on the colloidal suspensions (particle size between 5 and 12 nm). The slow decrease of the ZFC-FC curves and the hysteresis curve at room temperature implies a broad distribution of the size of the particles. This latter result indicates that some aggregation of smaller particles occurred during drying or annealing.

Conclusion

This paper demonstrates that microcontact printing (μCP) and capillary filling (CF) can be used to direct the deposition of metal oxides in patterns on a surface with feature sizes of microns. Selective wetting of a surface previously patterned by μCP allowed control of the deposition of iron oxides. Patterning of the substrate with the iron oxides was done either by deposition of magnetite from colloidal solution or by precipitation of the oxide from previously deposited drops of water containing iron(III) salt. The composition of the hydrophilic SAM had only a minor influence on the deposition of the iron oxides. The size of the metal oxide patterns was limited by the size of the patches that could be made with the μCP technique (about 0.5 μm); increases in the resolution of μCP will lead to decreases in the size of the areas of patterned iron oxides. Selective wetting of patterned substrate surfaces was also used for the direct deposition of iron oxides from solution by ferrite plating. Whereas the first two methods are well suited to deposit metal oxides in small, closed areas, ferrite plating—such as capillary filling—also allowed the deposition of continuous, interconnected structures of iron oxide.

Although there are still difficulties in an accurate and reproducible control of the shape, the thickness, and the roughness of the deposited magnetic material, our results clearly show that μCP and CF offer a convenient, experimentally simple, low-cost way for the fabrication of inorganic structures on the (sub)micron scale. Some deficiencies observed in the patterns clearly arise from difficulties in the processing. Improvements of the patterning can be expected from automatization of the stamping process, protection of the sample from any vibrations during the drying process, or the exclusion

of dust during the patterning process. Other deficiencies, particularly the shrinkage of the deposited area upon drying, result from a lack of specific interactions between the particles and the SAM; any deposition process governed by selective wetting of the SAM rather than by specific interactions between the surface and the material that should be deposited will have similar limitations in the edge resolution.

The magnetic properties of the deposited iron oxides were studied by magnetic force microscopy and by magnetic measurements. The magnetite particles that had been deposited in these experiments were too small to support a permanent magnetization, and showed superparamagnetic behavior. Annealing at high temperature and/or using bigger particles of ferrite would be necessary to produce ferromagnetic behavior in the deposited dots. A decrease in the size of the dots of the deposited magnetite to about 100 nm together with a significant improvement in the crystallinity of the particles would be necessary to prepare single magnetic domains that are a basic requirement for using each dot as a single bit in a memory device.

Acknowledgment. This work was supported in part by the ARO Multidisciplinary University Research Initiative, Award DAAH04-95-1-0102. It used MRSEC shared facilities supported by the NSF under Award DMR-9400396. S.P. gratefully acknowledges the NATO and the Commissariat à l'Energie Atomique (Saclay, France) for financial support. P.C.H. gratefully acknowledges a postdoctoral fellowship from the Swiss National Science Foundation. S.P. and P.C.H. thank Yuanchang Lu for his help with the instrumentation at the MRSEC.

CM950587U